Anisaxins, helical antimicrobial peptides from marine parasites, kill resistant bacteria by lipid extraction and membrane disruption

Tomislav Rončević[a,*], Marco Gerdol[b], Mario Mardirossian[c], Matko Maleš[d], Svjetlana Cvjetan[e], Monica Benincasa[b], Ana Maravić[a], Goran Gajski[f], Lucija Krce[g], Ivica Aviani[g], Jerko Hrabar[e], Željka Trumbić[h], Maik Derks[i,j], Alberto Pallavicini[b,k], Markus Weingarth[i], Larisa Zoranić[g], Alessandro Tossi[b], Ivona Mladineo[l,*]

[a] *Department of Biology, Faculty of Science, University of Split, Ruđera Boškovića 33, Split 21000, Croatia*
[b] *Department of Life Sciences, University of Trieste, Trieste 34127, Italy*
[c] *Department of Medical Sciences, University of Trieste, Trieste 34125, Italy*
[d] *Faculty of Maritime Studies, University of Split, Split 21000, Croatia*
[e] *Laboratory for Aquaculture, Institute of Oceanography and Fisheries, Split 21000, Croatia*
[f] *Mutagenesis Unit, Institute for Medical Research and Occupational Health, Zagreb 10000, Croatia*
[g] *Department of Physics, Faculty of Science, University of Split, Split 21000, Croatia*
[h] *University Department of Marine Studies, University of Split, Split 21000, Croatia*
[i] *NMR spectroscopy, Bijvoet Centre for Biomolecular Research, University of Utrecht, Utrecht 3584CH, The Netherlands*
[j] *Membrane Biochemistry and Biophysics, Bijvoet Centre for Biomolecular Research, Department of Chemistry, Utrecht University, Padualaan 8, Utrecht 3584 CH, The Netherlands*
[k] *Oceanography Division, Istituto Nazionale di Oceanografia e di Geofisica Sperimentale - OGS, Trieste, Italy*
[l] *Laboratory of Functional Helminthology, Biology Centre Czech Academy of Sciences, Institute of Parasitology BC CAS, Branisovska 31, Ceske Budejovice 37005, Czech Republic*

ARTICLE INFO

Article history:
Accepted 14 April 2022

Keywords:
α-helical antimicrobial peptides
Anisakis
Lipid extraction
Molecular leakage
Multi-drug resistant bacteria
Parasites

ABSTRACT

An infecting and propagating parasite relies on its innate defense system to evade the host's immune response and to survive challenges from commensal bacteria. More so for the nematode *Anisakis*, a marine parasite that during its life cycle encounters both vertebrate and invertebrate hosts and their highly diverse microbiotas. Although much is still unknown about how the nematode mitigates the effects of these microbiota, its antimicrobial peptides likely play an important role in its survival. We identified anisaxins, the first cecropin-like helical antimicrobial peptides originating from a marine parasite, by mining available genomic and transcriptomic data for *Anisakis* spp. These peptides are potent bactericidal agents *in vitro*, selectively active against Gram-negative bacteria, including multi-drug resistant strains, at sub-micromolar concentrations. Their interaction with bacterial membranes was confirmed by solid state NMR (ssNMR) and is highly dependent on the peptide concentration as well as peptide to lipid ratio, as evidenced by molecular dynamics (MD) simulations. MD results indicated that an initial step in the membranolytic mode of action involves membrane bulging and lipid extraction; a novel mechanism which may underline the peptides' potency. Subsequent steps include membrane permeabilization leading to leakage of molecules and eventually cell death, but without visible macroscopic damage, as shown by atomic force microscopy and flow cytometry. This membranolytic antibacterial activity does not translate to cytotoxicity towards human peripheral blood mononuclear cells (HPBMCs), which was minimal at well above bactericidal concentrations, making anisaxins promising candidates for further drug development.

Statement of significance

Witnessing the rapid spread of antibiotic resistance resulting in millions of infected and dozens of thousands dying worldwide every year, we identified anisaxins, antimicrobial peptides (AMPs) from ma-

* Corresponding authors.
E-mail addresses: troncevic@pmfst.hr (T. Rončević), ivona.mladineo@paru.cas.cz (I. Mladineo).

rine parasites, *Anisakis* spp., with potent bactericidal activity and selectivity towards multi-drug resistant Gram-negative bacteria. Anisaxins are membrane-active peptides, whose activity, very sensitive to local peptide concentrations, involves membrane bulging and lipid extraction, leading to membrane permeabilization and bacterial cell death. At the same time, their toxicity towards host cells is negligible, which is often not the case for membrane-active AMPs, therefore making them suitable drug candidates. Membrane bulging and lipid extraction are novel concepts that broaden our understanding of peptide interactions with bacterial functional structures, essential for future design of such biomaterials.

1. Introduction

The rapid emergence of multi-drug resistant bacteria contributes to millions of people being infected each year and thousands dying worldwide [1]. Drugs discovered during the "golden age" of antibiotics, in the 1960s and 70s and even more recently are being overwhelmed by the surge in antimicrobial resistance, which demands the development of new classes with alternative killing mechanisms, but in fact faces a reduced interest by the pharmaceutical industry. The number of promising compounds in the developmental pipeline is quite limited [2], and only a handful of these have truly different mechanisms of action. As of 2017, the World Health Organization has shortlisted a set of bacterial species for which potent new drugs are critically required, including carbapenem- and 3rd generation cephalosporin-resistant *Acinetobacter baumannii, Pseudomonas aeruginosa* and *Enterobacteriaceae* [3].

Antimicrobial peptides (AMPs) are promising candidates to help mitigate antimicrobial resistance. These multifunctional effector molecules are produced as part of the innate immune systems of higher organisms and have a direct antimicrobial activity sometimes associated with immunomodulatory properties. They generally show a broad-spectrum efficacy towards Gram-negative and Gram-positive bacteria, that includes multidrug-resistant strains [4,5], and their mode-of-action is typically based on non-specific interactions with the bacterial membrane, leading to its disruption. This seems to discourage the development of sustained bacterial resistance [6]. However, their use outside of their physiological context, as externally administered therapeutic agents, is hindered by a relatively low stability *in vivo*, as well as often unacceptable levels of toxicity towards host cells [7]. This is one of the main reasons that few AMPs have reached the later stages of clinical trials, despite of sustained efforts to develop them.

The many natural AMPs that have been identified rarely have biological activities that are already suitable for their use as therapeutic agents, and it seems quite difficult to redesign them to obtain such properties [7]. This despite the fact that they are widespread and effective in nature as endogenous antibiotics, and there is a seemingly inexhaustible supply of such peptides. According to the $CAMP_{R3}$ database, which includes more than 8000 entries, the majority of identified AMPs originates in animal species [8]. However, those from parasitic helminths (Nematoda and Annelida [9]) account for a very small number, unlikely to gain them a spotlight in the drug development agenda. Parasitism is considered by biologists to be a highly successful life strategy, that has evolved independently multiple times, and is a driving force for generating genetic diversity, making it an underrated source of useful pharmacophores [10]. During their evolution, parasitic organisms have adopted a variety of traits associated with survival, based on effectively evading their host's immune systems and reaching a *modus vivendi* with the host's microflora (endo- and/or ectosymbiotic archaea, bacteria, viruses, as well as eukaryotic microbes). Parasite-host interactions are considered to be strongly influenced by the microbiomes of both the parasite and the host, which has led to the concept of the "holobiont" - a composite of multiple constitutive organisms [11].

Given the extraordinary versatility helminths show in adapting to a variety of niches during their complex life cycles [12], which promotes their ability to modulate the hosts' immune response [13], parasite-derived AMPs may be a promising source of potential drug leads that are effective without being excessively toxic. We focused our attention on *Anisakis* spp., zoonotic nematodes whose life cycle begins in the gastric chambers of the final host, a toothed whale. Eggs expelled into seawater are ingested by intermediate hosts; crustaceans and small fish, which are then preyed upon by larger fish and cephalopods. In these so-called paratenic hosts, the larvae moult into the third-stage (L3) and return to the final host, which feeds on the infected paratenic hosts (**Fig. S1**) [14]. Paratenic host larvae remain in an indefinitely dormant state (paratenesis), while the adult stage in the final host causes chronic inflammatory effects, but these are not considered to be life threatening [15]. Humans can also become accidentally infected by L3, by consuming uncooked seafood, and develop gastric, intestinal, ectopic and gastroallergic reactions. They may remain asymptomatic, but become sensitised to parasite allergens [16]. Humans are in any case considered accidental hosts, as L3 cannot reach adulthood in any terrestrial mammalian species [17].

The increasing availability of -omics resources related to nematodes has prompted us to mine for and characterize AMPs from marine nematodes of the genus *Anisakis*. Herein we describe the characterization of five antimicrobial peptides, we have called anisaxins, with respect to their toxicity, stability and *in vitro* activity against a panel of Gram-negative and Gram-positive bacteria, focusing on their mode of action - especially peptide/membrane interactions, using biochemical, biophysical and *in silico* methods.

2. Materials and methods

2.1. Peptide identification

The *Anisakis simplex sensu lato* genome assembly, version ASM90057681v [18] and raw RNA-sequencing data for *A. simplex* and *A. pegreffii* [19] were used for data mining. Sequencing data was imported into the CLC Genomics Workbench v.11 environment (Qiagen, Hilden, Germany) and trimmed to remove Illumina sequencing adapters, low quality regions and ambiguous nucleotides. The resulting data was *de novo* assembled with Trinity v2.8.6 as per default parameters.

Known cecropin-like sequences from Nematoda were retrieved from public databases and used as queries for tBLASTn searches against the two transcriptomes, setting the e-value threshold for detection to 0.05. These included the previously reported cecropins from *Ascaris suum, Ascaris lumbricoides* and *Toxocara canis* [20], as well as those resulting from virtual translations of gene models from the recently released *T. canis* genome [21]. The retrieved nucleotide sequences from *A. simplex* and *A. pegreffii* were quality-checked by assessing that the entire CDS was covered in a uniform way by RNA-seq reads, virtually-translated and aligned with the sequences of the known cecropins listed above (**Fig. S2**). This,

together with the use of SignalP 5.0 [22], enabled the detection of the signal peptide region, as well as of the mature peptide C-terminal cleavage site based on previously reported information by other authors [20].

The complete *in silico* validated cDNA sequences were subsequently used as BLASTn queries against the *A. simplex sensu lato* genome, which allowed the confirmation of two annotated genes (i.e., ASIM_LOCUS17004 and ASIM_LOCUS10039) and the detection of one additional complete gene. The latter was manually annotated based on the alignment between the cDNA and genomic DNA sequences, with splicing donor and acceptor sites being refined with Genie [23]. The expression levels of all the different variants identified in the two species were assessed based on the mapping of the trimmed RNA-sequencing reads against the reference cDNA sequences. This was performed using the CLC Genomics Workbench v.11 *map reads to reference* tool, setting the length fraction and similarity fraction parameters to 0.75 and 0.98, respectively. Considering that all the cecropin cDNAs displayed a similar length, the comparison between the expression levels of the different isoforms was evaluated by calculating Count Per Millions (CPM).

2.2. A. pegreffii *transcriptomics analysis*

A detailed description of the experimental design of Sprague-Dawley rat infections was published in Trumbić et al. [17]. *A. pegreffii* infective third-stage larvae (L3) were collected when perforating rat tissues and designated as migrating L3 (successful infection), or free in the intestinal lumen/ entrapped within rat feaces and designated as non-migrating L3 (unsuccessful infection). Experimental design for European seabass *Dicentrarchus labrax* infection followed the same approach as for rat, except that L3 were designated as non-migrating (same as in rat - unsuccessful infection), post-migrating (L3 collected while migrating through visceral cavity in model fish - successful infection) and spiralized (L3 spiralized on visceral organs in model fish - successful infection). Prior to both experiments, L3 spiralized on visceral organs of wild fish (*Micromesistius poutassou*) used as an inoculant for the experimental infections, were also collected and designated as pre-infection.

Extraction of *Anisakis* RNA, library preparation for Illumina sequencing and RNA-Seq reads pre-processing followed the pipeline described in Trumbić et al. [17]. Briefly, reads were screened for host contaminants by mapping against their respective host genomes (rat and seabass) and reads that failed to map were concatenated across all samples into a single set of inputs and used to reconstruct a reference transcriptome using Trinity v2.8.6. [24] as per default parameters. Trinotate v3.1.1 [25] annotation suite was used to annotate the transcriptome across various functional databases. Paired-end reads of each sample were mapped to the reference transcriptome and abundances were estimated using RSEM v1.3.1 [26]. Gene level estimated counts were imported into R v3.6.3 [27] and differential analysis of gene expression was performed using DESeq2 package [28]. A generalized linear model was fitted for each gene with multi-factor design that included state (migrating vs non-migrating) and host as fixed effects. Differentially expressed genes (DEGs) were identified at Benjamini-Hochberg false discovery rate (FDR) < 0.05. TPM values were calculated for each transcript and used to visualize relative contribution of anisaxins' expression in each host.

Although between-host comparisons should be taken with precaution as the samples were sequenced on different RNAseq runs, a couple of samples from a third run clustered primarily by their phenotype suggesting much of the captured variance is biologically relevant (**Fig. S3**).

2.3. Peptide synthesis

The mature peptide regions for selected anisaxins were synthesized by ProteoGenix (Schiltigheim, France), purified to >98% purity by RP-HPLC (LC3000, Beijing Chuangxin Tongheng Science and Technology, Beijing, China; 5 µm column, 4.6 × 250 mm) using a 25–75% acetonitrile/0.1% TFA gradient in 25 min at a 1 ml/min flow rate (**Fig. S4**) and the sequences confirmed by ESI-MS operated in positive mode and with 0.2 mL/min flow (LCMS-2020, Shimadzu, Kyoto, Japan). Peptide stock solutions were prepared by dissolving accurately weighed aliquots of peptide in doubly distilled water, and the concentration further verified by using the extinction coefficients at 214 nm, calculated as described by Kuipers and Gruppen [29].

2.4. Circular dichroism

Peptide conformation and its variation in membrane-like environments was assessed from the CD spectra, as obtained on a J-710 spectropolarimeter (Jasco, Tokyo, Japan). Spectra were the accumulation of three scans measured in *(i)* SPB solution ($NaH_2PO_4 \times H_2O$: Na_2HPO_4 0.39:0.61, v/v, 10 mM, pH 7), *(ii)* 50% trifluoroethanol (TFE) in 10 mM SPB, and *(iii)* dodecyl sulphate (SDS) micelles (10 mM SDS in SPB). The helix content was determined as $[\theta]^{222} / [\theta]^{\alpha}$, where $[\theta]^{222}$ was the measured molar residue ellipticity at 222 nm under any given condition and $[\theta]^{\alpha}$ is the molar ellipticity for a perfectly formed alpha helix of the same length, estimated as described by Chen et al. [30].

2.5. Bacterial strains and antibacterial assays

In vitro antimicrobial testing of anisaxin peptides was carried out on both Gram-negative laboratory strains and multi-drug resistant clinical isolates (c.i.) (for details please see Table S1 in Roncevic at al. [31] and Tables S1 and S2 in Juretic et al. [32]) including *Escherichia coli* ATCC 25922, *Klebsiella pneumoniae* ATCC 13883, *A. baumannii* ATCC 19606 and *P. aeruginosa* ATCC 27853. *Staphylococcus aureus* ATCC 29213 was used as a representative of Gram-positive bacteria. Minimal inhibitory concentrations (MIC) were assessed using the serial two-fold microdilution method following Clinical and Laboratory Standards Institute protocols [33]. Bacteria were cultured in fresh Mueller Hinton broth (MHB) to the mid exponential phase, and then added to serial dilutions of anisaxins to a final bacterial load of 5×10^5 CFU/mL of cells in 100 µL per well, incubated at 37 °C for 18 h. MIC values were visually determined as the lowest consensus concentration value of the peptide showing no detectable bacterial growth, for an experiment performed at least in triplicate.

For determination of the minimal bactericidal concentration (MBC), 4 µL of bacterial suspensions from the wells corresponding to MIC, 2 × MIC, and 4 × MIC were plated on MH agar plates. Plates were incubated for 18 h at 37 °C to allow the viable colony counts and the MBC was determined as the peptide concentration causing no visible growth.

Bacterial viability was additionally assessed on *E. coli* ATCC 25922 with the time-killing kinetics assay. Bacteria were grown at 37 °C in fresh MHB to the mid-exponential phase (1×10^7 - 1×10^8 CFU/mL) and peptides added at concentrations corresponding to ½ × MIC and 2 × MIC. These suspensions were incubated for 4 h and aliquots were extracted at the specified time points and serially 10-fold diluted in phosphate buffer before plating on MH agar overnight at 37 °C, and then carrying out viable cell counts.

2.6. Solid state NMR (ssNMR) of peptide-membrane interactions

Unilamellar vesicles were prepared with zwitterionic 1,2-dioleoyl-*sn*-glycero-3-phosphocholine (DOPC) and anionic DOPC/DOPG (1,2-dioleoyl-*sn*-glycero-3-phosphoglycerol) (1:1 molar ratio) in 20 mM HEPES (pH 7.2) by the extrusion technique and using filters with a 200 nm cut off [34]. Peptides were added to the vesicles to a final molar ratio of 1:50 peptide/lipid. The vesicles were collected by ultracentrifugation and subsequently spun down into 3.2 mm NMR (Bruker, Billerica, Massachusetts, USA) rotors. Static ^{31}P ssNMR spectra were acquired at 500 MHz magnetic field (11.7 T) and a sample temperature of 280 K. SPINAL64 proton decoupling [35] was applied with 50 kHz amplitude. The resulting ^{31}P powder patterns were apodised with 50 Hz exponential line-broadening and baseline corrected.

2.7. Membrane integrity assay

The integrity of bacterial membranes after exposure to anisaxin peptides was assessed as percentage of propidium iodide (PI) positive cells, using a Cytomics FC 5000 flow cytometer (Beckman-Coulter, Inc., Fullerton, CA). Measurements were carried out on *E. coli* ATCC 25922 cultured in MHB to the mid-logarithmic phase. After incubation, propidium iodide (PI) was added to the bacterial suspension (1×10^6 CFU/mL) at a final concentration of 15 µM, whereas the peptides (final concentration 0.125–0.5 µM) were added just before the beginning of the analysis. The measurements were taken at 15, 30 and 60 min and the cells incubated in MHB without peptides were used as a negative control. The analysis was performed with the FCS Express3 software (De Novo Software, Los Angeles, CA, USA) and the data are the average from at least three different experiments.

2.8. Atomic force microscopy (AFM) and fluorescence imaging

To visually discern the effect of peptides on the bacterial membrane, AFM measurements were carried out using a Nanowizard IV system (JPK/Bruker, Berlin, Germany) operating in the quantitative imaging (QI) mode utilizing the MLCT-E probes (Bruker, Billerica, USA), mounted on an inverted optical fluorescence microscope IX73 (Olympus, Tokyo, Japan). The extend/retract speed was up to 200 µm/s while the setpoint was kept between 0.82 nN and 2 nN. The pre- and post-treatment AFM data were obtained at the same force setpoint for each data set. Each height image had the resolution of 256 × 256 pixels. The AFM data processing was carried out using the JPK data processing software.

Measurements were carried out on the *E. coli* reference strain cultured in MHB to the mid-logarithmic phase. A 50 µL aliquot of bacterial suspension was transferred to Petri dishes (WPI, Sarasota, USA) and coated with the Cell-Tak (Corning, NY, USA) solution prepared as previously reported [36,37]. In order to eliminate non-adhered and loosely adhered cells the culture was thoroughly rinsed with MHB ten minutes post application, ensuring that the sample did not dry out while rinsing. All AFM measurements were obtained in MHB at 37 °C.

Initially, a group of untreated cells was chosen at the bright field image followed by AFM imaging. The same region was imaged with AFM at least two times to make sure that the chosen cells were viable. The AFM measurements of peptide treated cells at 4 × MIC concentration would start about 30 min after the treatment. The post-treatment measurements reported here were taken 90 min after the treatment.

The sample preparation for fluorescence imaging was done immediately after the AFM measurements. The growth medium was replaced with the physiological saline solution and the cells stained using the LIVE/DEAD BacLight Bacterial Viability Kit L7012 (Invitrogen, Carlsbad, USA). PI (which dyes ruptured cells) and SYTO 9 (which dyes all cells) were mixed in the equal volumes and 3 µl of this mixture was added per ml of the cell culture. The florescence data were obtained 3.5 h after the treatment and 30 min after adding the fluorescence dyes. Fluorescence images have been obtained on the exact same region that was imaged by the bright field and AFM.

2.9. Molecular dynamics (MD) simulations

Simulations were carried out using Gromacs, version 2021.0 [38], with the CHARMM36 force field [39] and TIP3P model for water molecules [40]. Anisaxin-2S was used in a closed surrounding consisting of a negatively charged lipid bilayer immersed in water. The membrane bilayer consisted of 1-palmitoyl-2-oleoyl-*sn*-glycero-3-phosphoethanolamine (POPE) and 1-palmitoyl-2-oleoyl-*sn*-glycero-3-phospho-(1′-*rac*-glycerol) (POPG) lipids in a 3:1 mixing ratio (576:192 lipid molecules) modeled on the *E. coli* membrane [41]. The solvated membranes (in the absence of peptides) were equilibrated for 0.6 ns at $T = 340$ K and $p = 1$ ATM, and the thermal stability was verified. The α-helical peptide structure, used as the initial input in MD set-ups, was obtained using the QUARK server [42]. The peptides' charge was defined for pH 7, considering a charged N-terminal amine but neutral amidated C-terminus. A water layer of 5 nm thickness was added above and below the membrane bilayer, which led to ∼100 water molecules per lipid. The system was neutralized with addition of Na^+ ions. The initial conformations were prepared by the CHARMM-GUI membrane modeler [43].

Simulations were performed with six or twelve peptides embedded in the membrane surface, to mimic a high local peptide density, where peptide molecules are located at a short distance from each other, creating a favorable condition for their assembly (following Miyazaki et al. [44]). Simulations were carried out for 1 µs. Equilibration was according to CHARMM-GUI recommendations [45], consisting of isothermal-isochoric (NVT) dynamics in the first two steps, followed by NpT dynamics in next four steps, where various restraints were applied at the fixed temperature of 340 K. The production runs were in the isothermal-isobaric (NpT) ensemble conditions, and $T = 340$ K and $p = 1$ ATM were imposed using the Nose-Hoover thermostat and Parrinello–Rahman barostat, with a 1.0 ps time constant for the temperature and a 5.0 ps time constant for the pressure (compressibility equal to 4.5 10^{-5} bar) [46,47]. The leapfrog integrator time step was fixed at 2 fs, and the bonds were handled by the LINCS option [48]. The particle-mesh-Ewald method [49] was used for calculation of the electrostatic interaction with coulomb cut-off set to 1.2 nm and the van der Waals cut-off set to 1.2 nm, with the force-switch set to 1.0 nm.

2.10. Cyto/genotoxicity assays

The cyto- and genotoxic effects of anisaxin peptides were evaluated in human peripheral blood cells (HPBCs) obtained from two healthy young male donors by antecubital venipuncture into heparinized vacutainers under aseptic conditions. Subjects gave informed consent to participate in this study that was approved by the Ethics Committee of the Institute for Medical Research and Occupational Health, Zagreb, complying to the Declaration of Helsinki. The whole blood samples were exposed to increasing concentrations of peptides (0, 1.5, 3, 6, 12, 25, 50 and 100 µM) for 4 and 24 h periods and human peripheral blood mononuclear cells (HPBMCs) for the cytotoxicity assessment were obtained by histopaque density gradient centrifugation. Cells were mixed with acridine orange (AO) and ethidium bromide (EtBr) (1:1; v/v) and

a total of 100 cells per repetition were examined with the epifluorescence microscope (Olympus BX51, Tokyo, Japan). Quantitative assessments were made by determining the percentage of live (green fluorescence of nuclei) and dead cells (red fluorescence of nuclei) [50].

Genotoxicity was determined employing the alkaline comet assay with minor modifications [51,52] following recommendations for describing comet assay procedures and results [53]. After exposure to peptides as described above, the whole blood (5 µl) was mixed with 0.5% low melting point (LMP) agarose and added to fully frosted slides pre-coated with 0.6% normal melting point (NMP) agarose. Cells were lysed overnight (2.5 M NaCl, 100 mM $EDTANa_2$, 10 mM Tris, 1% sodium sarcosinate, 1% Triton X-100, 10% DMSO, 4 °C, pH 10), placed into alkaline solution to allow DNA unwinding (20 min, 300 mM NaOH, 1 mM $EDTANa_2$, 4 °C, pH 13) and subsequently underwent electrophoresis (20 min, 1 V/cm). After neutralizing the alkaline solution (5 min, 0.4 M Tris buffer, pH 7.5), cells were stained with EtBr (10 µg/ml) and observed at 250 × magnification on an epifluorescence microscope (Zeiss, Göttingen, Germany) with a black and white camera. For each slide, 100 randomly captured comets were examined by an image analysis system (Comet Assay II; Perceptive Instruments Ltd., Haverhill, Suffolk, UK) and the percent of tail DNA was used to assess the level of DNA damage.

2.11. Statistical analysis

The difference in the cell viability between control and treated samples was evaluated using the χ2-test. Comet assay results were evaluated using the Statistica 13.2 software package (Dell Inc., USA). In order to normalize the distribution and equalize the variances of the comet assay data, a logarithmic transformation was applied. Multiple comparisons between groups were affected by ANOVA on log-transformed data. *Post-hoc* analyses of differences were carried out using the Scheffé test. Data were considered statistically significant at $P < 0.05$.

Other methods, described in Supplementary information, include *DNA-binding analysis, DNA analysis of individual colonies by pulsed field gel electrophoresis (PFGE), Transcription/translation assay and Pharmacokinetic assay*.

3. Results

3.1. Peptide sequences

We were inspired by reports that peptides of the cecropin family are present in Nematoda such as *Ascaris* and *Toxocara* to screen available *Anisakis* spp. genomes and transcriptomes using known nematode cecropin sequences as queries [20]. To our knowledge, none had yet been identified in zoonotic parasitic nematodes from the marine environment. This resulted in the identification of 14 potentially interesting peptide precursor sequences (**Fig. S2**), which were filtered and selected for synthesis and further testing based on *(i)* evidence of expression, to discriminate functional genes from possible pseudogenes; *(ii)* a net positive charge, which is a functionally relevant hallmark of AMPs; *(iii)* the largest possible molecular diversity. This narrowed the set to five cecropin-like peptide sequences, named anisaxin 1-4, that are identical in *A. simplex* and *A. pegreffii*, with the exception of the orthologous sequences for anisaxin-2, with a one-residue difference, so they are respectively identified as anisaxin-2S and -2P (Table 1). Two ansaxin-4 paralogs (anisaxin-4.1 and anisaxin-4.2) were also identified in *A. pegreffii* and *A. simplex* (**Fig. S2**), however, having identical mature sequences we refer to these simply anisaxin-4.

Sequence comparisons indicate that, for the most part, the mature region is quite conserved, with variations mainly limited to 4 positions (see Table 1), and this extends also to orthologues from *Toxocara* [20]. The N-terminal signal peptide region and C-terminal pro-peptide region are less conserved (see **Fig. S2**). All of the selected peptides showed physico-chemical properties that are favorable for potent antimicrobial activity, a net charge was +6 (with the exception of anisaxin-3, +5), and the hydrophobicity ranging from -1.6 to -2.1, indicating that polar and hydrophobic residues are well balanced (Table 1). The relative hydrophobic moment of around 0.3 based on a helical conformation, however, indicates that these helices are only moderately amphipathic, and this is confirmed also by helical wheel projections (see **Fig. S5**). In this respect, conserved glutamate residues in positions 11 and 20 are placed in such a manner as to stabilize the helix once it forms side-chain salt-bridging being spaced 3 or 4 residues N- or C-terminal to positively charged ones.

3.2. Anisaxins expression in A. pegreffii

We have observed that *A. pegreffii* regulates transcription of eight AMPs during accidental (Sprague Dawley rat model) and paratenic hosts (seabass model) infection (Fig. 1), which include the peptides selected for synthesis and further characterization. The peptides' expression (full cDNA sequence used as a reference) was not found to be significantly different between larvae that successfully infected a host (migrating, post-migrating or spiralized larvae) and faecally-expelled larvae unable to infect a host (non-migrating larvae). In contrast, a striking effect on expression was related to the host itself (Fig. 1, **Table S1**). Anisaxin-1 to -4.1 seem to be generally expressed in all three hosts, where anisaxin-1 is preferentially expressed in seabass, anisaxin-3 in both the experi-

Table 1
Sequence and physico-chemical properties of anisaxins and similar peptides.

Peptide	Name	Sequence	Charge	H[a]	H[rel b]
		----:----|----:----|----:----|-			
Anisaxin-1	A-1	SWLSKTYKKLENSAKKRIAEGIAIALRGGPR	+6	-2.1	0.31
Anisaxin-2S	A-2S	SWLSKTWKKLENSGKKRIAEGIAIALKGGLR	+6	-1.6	0.30
Anisaxin-2P	A-2P	SWLSKTWKKLENSGKKRIAEGIAIALKGGAR	+6	-1.9	0.35
Anisaxin-3	A-3	SWLSKTAKKLENSAKKRIAEGIAIAIQGGPR	+5	-2.1	0.28
Anisaxin-4	A-4	GWLSKTWKKLENSAKKRIAEGIAIAIRGGPR	+6	-1.8	0.34
As-cecropin [20]	*As*-Cec	SWLSKTAKKLENSAKKRISEGIAIAIQGGPR	+5	-2.1	0.29
Melittin [53]	Mel	GIGAVKLVLTTGLPALISWIKRKRQQ-NH_2	+6	0	0.48

a) Hydrophobicity, calculated using the CCS scale [55].
b) Hydrophobic moment relative to a perfectly amphipathic helical peptide of 18 residues. Conserved positions are shaded gray.

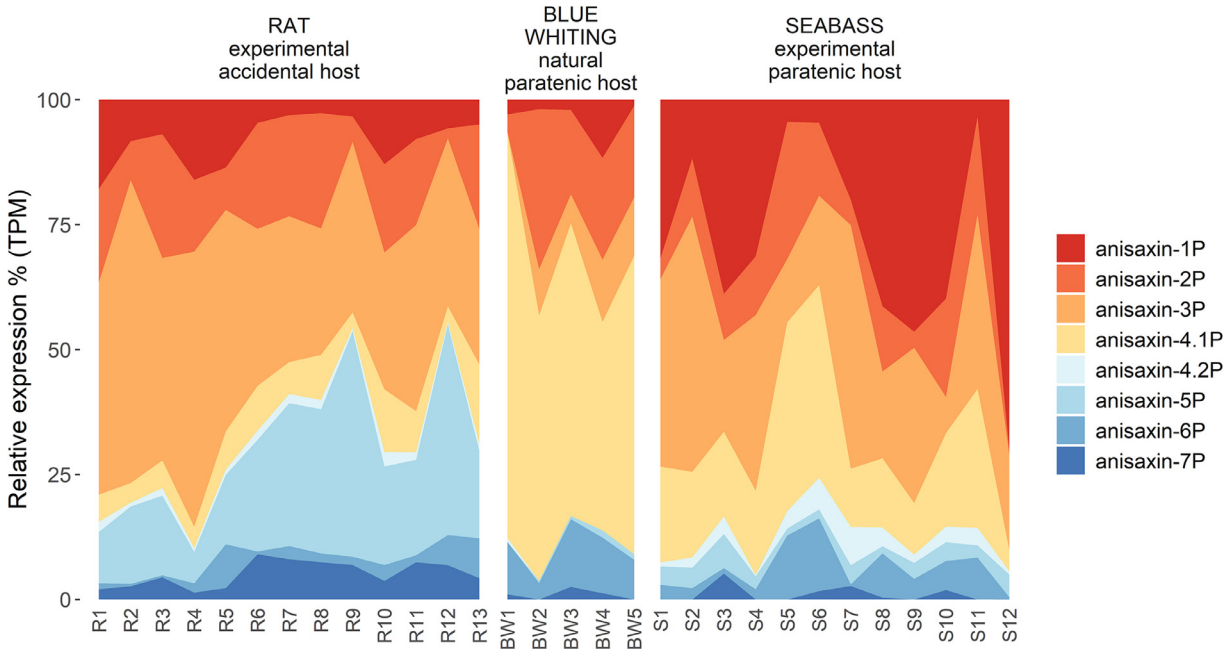

Fig. 1. Relative expression of cecropin homologues identified in transcriptomes of *A. pegreffii* L3 larvae found in wild fish, blue whiting (BW), or in a rat (R) or seabass (S) experimentally infected with L3 sourced from wild fish. Rat is an experimental model of accidental infection otherwise characteristic for humans, and seabass is an experimental model of paratenic infection typical for marine fish that serve to transfer L3 to its final host, a marine mammal. For each sample denoted on the x axes (R1-13, BW1-5, S1-12), relative expression of each anisaxin in an anisaxin pool is depicted on the y axes as % of normalized counts (TPM, Transcripts Per Million). To outline the predominance of transcripts, relative expression profiles are depicted as an area plot.

mental hosts (paratenic seabass and accidental rat), while anisaxin-2 and especially ansiaxin-4.1 predominate in the larvae resting in natural paratenic host (blue whiting) (Fig. 1). The other peptides from *A. pegreffii* (anisaxin-4.2, -6 and -7, see Fig. 1 and **Table S1**) are less expressed under all conditions and only anisaxin-5 is preferentially expressed in the accidental rat model of infection, but not in paratenic hosts, experimental or natural.

3.3. Secondary structure

The secondary structure of anisaxin peptides was evaluated using circular dichroism (CD) spectroscopy in different environments: *(i)* aqueous solution at neutral pH (SPB), *(ii)* anisotropic solvent conditions (50% TFE in 10 mM SPB) and *(iii)* a membrane-mimicking environment (SDS in 10 mM SPB). The spectra in aqueous buffer are typical of disordered conformations for all five peptides, whereas in the anisotropic environments they clearly suggest a transition to a helical conformation. This is somewhat more pronounced in 50% TFE compared to SDS micelles, but in both cases the shape of the spectra and in particular a $\theta^{208}/\theta^{222}$ ratio >1, suggests that the helices under these conditions are not stacked (Fig. 2) [56]. The helical wheel projections (see **Fig. S5**) suggest that an amphipathic helix could form in the more cationic N-terminal part of the peptide.

Comparing spectra suggests that anisaxin-2S and -3 have the most helical content (∼50% in TFE), followed by anisaxin-2P with ∼40%. Anisaxin-1 and -4, although having a similar primary structure to the other peptides, show the least structuring in all environments. This suggests that they have a reduced capacity to interact with membrane-like environments, or alternatively, that the interaction does not markedly alter their conformation.

3.4. Antibacterial activity

We tested the activity of anisaxin peptides against a panel of reference strains and drug-resistant clinical isolates (Table 2). The peptides were broadly active against Gram-negative bacteria and seemed equally active against reference strains and clinical isolates, with MIC values generally between 0.5 and 1 μM (sometimes as low as 0.25 μM, which is unusual for helical AMPs). This was observed in particular against *E. coli, K. pneumoniae* and *A. baumannii*, whereas *P. aeruginosa* showed the least susceptibility to these peptides, although the MIC value range is still appreciable (4 - 16 μM). Anisaxin-2S and -4, which were most active against the reference *P. aeruginosa* strain (MIC = 4 μM) also showed a better activity against some drug-resistant clinical isolates (MIC = 2 μM). With respect to *S. aureus,* a representative of Gram-positive bacteria, they were less potent, with MIC generally ranging from 16 to 64 μM or higher. Only anisaxin-2S and -4 showed a good activity against the reference *S. aureus* strain (MIC = 2-4 μM) but were inactive against clinical isolates. This could indicate selectivity towards Gram-positive bacteria.

The MBC (bactericidal) values against all tested strains, for all the tested peptides, were similar to the MIC values, suggesting that anisaxins are bactericidal rather than bacteriostatic (Table 2).

The antimicrobial potency of anisaxin peptides was further evaluated by determining their effect on bacterial growth kinetics using a time-kill assay at concentration both above and below the respective MIC values. They slowed the growth of the *E. coli* reference strain also at sub-MIC values, but the bacteria were eventually able to recover, and growth restarted after approximately 30 min post exposure (Fig. 3). At twice the MIC, growth inhibition was more pore permanent, and A-1 and A-2S in particular significantly reduced viable bacterial counts. It should be pointed out that, under the conditions required for these assays, the initial inoculates have bacterial concentrations three orders of magnitude higher than for MIC assays.

3.5. Peptide - membrane interaction

The ability of anisaxin peptides to interact with bacterial and/or model membranes was evaluated using static ^{31}P ssNMR, flow cy-

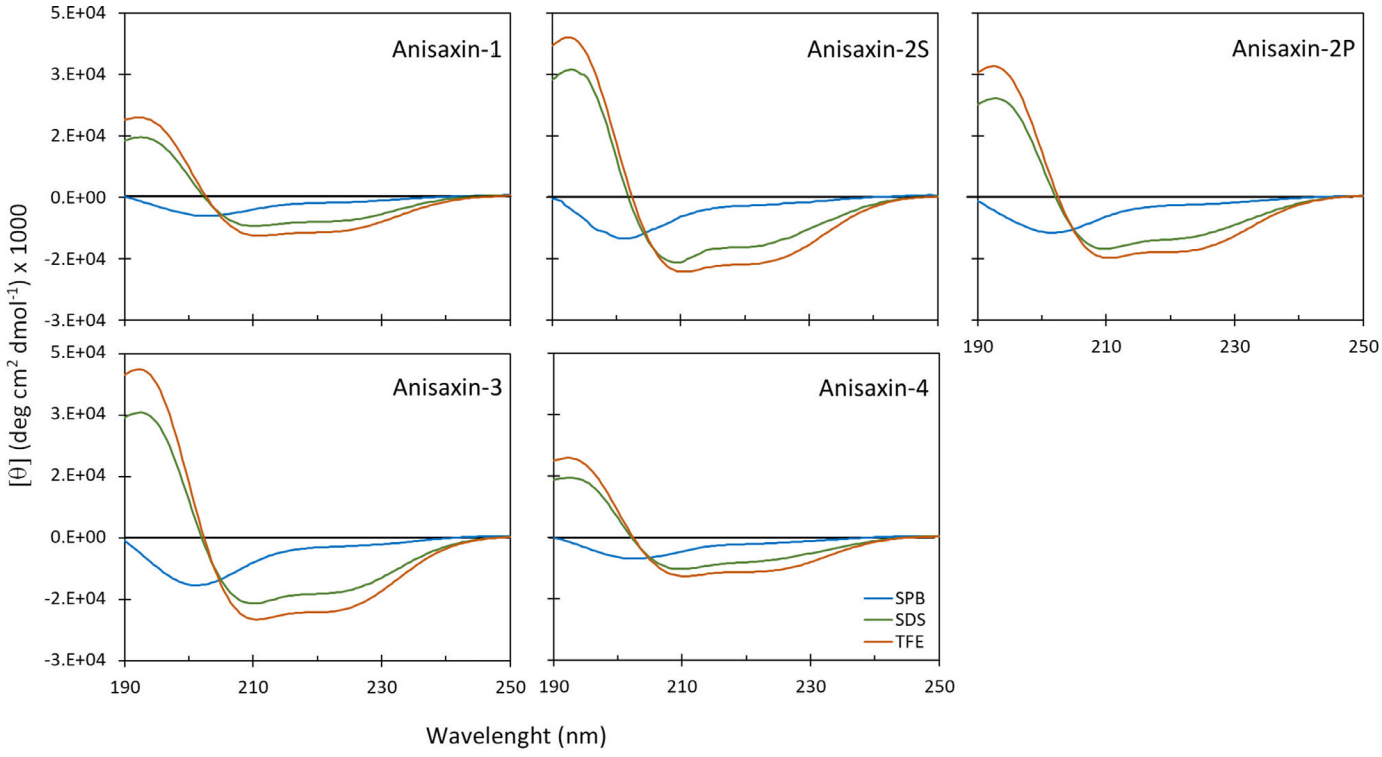

Fig. 2. CD spectra of anisaxin peptides in different environments. Spectra are the accumulation of three scans carried out with 20 μM peptide in SPB (sodium phosphate buffer), 10 mM SDS (sodium dodecyl sulphate micelles) in SPB or 50% TFE (trifluoroethanol) in SPB.

Table 2
Antimicrobial activity of anisaxin peptides in MHB expressed as MIC (μM) and MBC (μM).

Bacterial strain	Anisaxin-1		Anisaxin-2S		Anisaxin-2P		Anisaxin-3		Anisaxin-4	
	MIC	MBC	MIC	MBC	MIC	MBC	MIC	MBC	MIC	MBC
E. coli ATCC	1	1	0.5	0.5	0.5	0.5	0.25	0.25	0.5-1	0.5-1
E. coli c.i.	1-2	1-2	0.5	0.5	1	1	1	1	1	1
E. coli c.i. 2	2	2	1	1	1-2	1-2	1	1	1-2	1-2
K. pneumoniae ATCC	0.5-1	1	0.25	1	0.5-1	0.5-1	0.5-1	0.5-1	0.5	0.5
K. pneumoniae c.i.	1-2	1-2	0.5	0.5	1	1	1-2	1-2	1	1
K. pneumoniae c.i. 2	2-4	2-4	1	1	1-2	1-2	2	2-4	1-2	1-2
A. baumannii ATCC	1	1	0.25-0.5	0.5	0.5	0.5	0.5	0.5	1	1
A. baumannii c.i.	1	1	0.5	0.5	0.5	0.5	0.25	0.25	0.5-1	0.5-1
A. baumannii c.i. 2	1	1	0.5	0.5	1	1	0.5	0.5	1-2	1-2
P. aeruginosa ATCC	8	8-16	4	4-8	16	32	32	32	4	4
P. aeruginosa c.i.	4	4	1-2	2-4	4	8-16	4	4-8	2	2
P. aeruginosa c.i. 2	8	8	4-8	4-8	8	8	8	16	4	4
S. aureus ATCC	16-32	16-32	4	4	32-64	64	>64	NA	2	2
S. aureus c.i.	>64	NA	>64	NA	>64	NA	>64	NA	>64	NA
S. aureus c.i. 2	>64	NA	>64	NA	>64	NA	>64	NA	>64	NA

[NA] not applicable; [c.i.]clinical isolate.

tometry, atomic force microscopy (AFM) and fluorescence imaging. ^{31}P ssNMR spectra were measured for peptides in contact with either zwitterionic DOPC or negatively charged 1:1 DOPG/DOPC large unilamellar vesicles (LUVs). Static ^{31}P spectra of lipid membranes are dominated by chemical shift anisotropy resulting in powder patterns that are sensitive to the orientation and mobility of the lipid headgroups [57–59]. The comparison of spectra for LUVs in the presence and absence of peptide thereby allows to investigate the influence of the peptide on the phase, shape and the dynamics of the membranes (Fig. 4). Anisaxin-1, -2S, -2P and -4 had virtually no effect on the DOPC ^{31}P spectra, implying little or no binding interaction. Only anisaxin-3 caused a broadening of the powder pattern by approximately 8 ppm (1.6 kHz) at 10% peak height, indicating some modulation of the lipid headgroups. Interestingly, given that zwitterionic lipid membranes are to some extent representative of eukaryotic cell membranes, the pronounced interaction of anisaxin-3 with DOPC vesicles suggests that it might also interact with animal cell membranes, resulting in a higher toxicity. In stark contrast, anisaxin-1, -2S, -2P and -3 caused considerable change in the powder pattern of anionic vesicles, more representative of bacterial membranes, indicating that interactions with the lipid bilayers are markedly charge-dependent. For all these peptides, we observed a clear shift in the center of the DOPG/DOPC powder pattern, while the overall peak width was unaffected, suggesting they have a similar membrane binding mode. The clear charge dependence of binding indicates selective interaction of these cationic

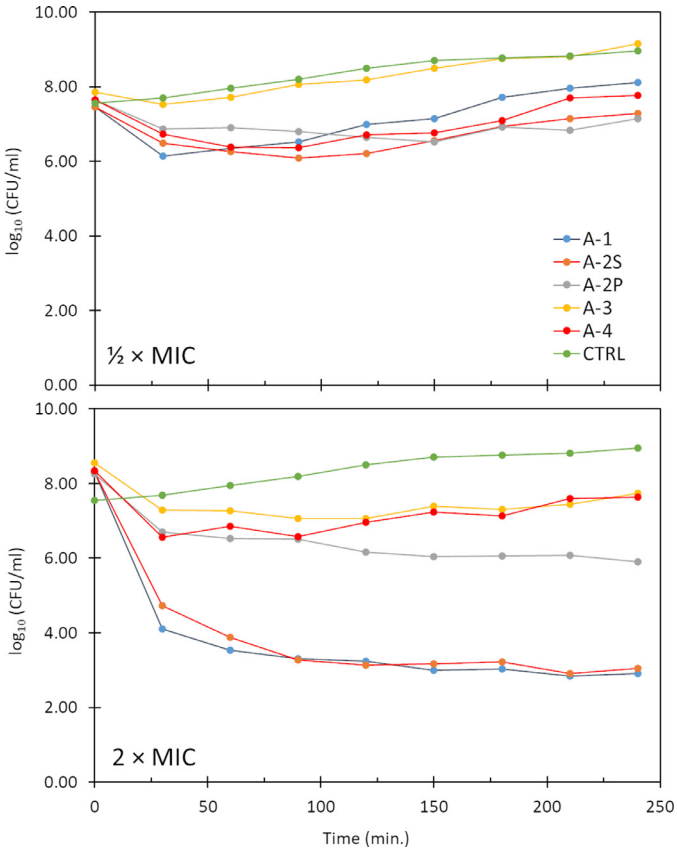

Fig. 3. Time-kill kinetics curve of *E. coli* ATCC 25922 after exposure to anisaxin peptides. Peptides were incubated with bacteria (1×10^7 - 1×10^8 CFU/mL in MHB) for 4 h at ½ × MIC and 2 × MIC. After the first 30 min of exposure to anisaxins there is a sudden drop in the number of bacteria, after which bacteria recover (except when treated with A-1 and A-2S at 2 × MIC). Data are the average from three independent experiments.

peptides with anionic bacterial membranes. In this case, the exception was anisaxin-4, for which only marginal broadening was observed, suggesting a different mode of action for this peptide that does not seem to correlate clearly with its net charge.

Some AMPs, such as indolicidin, interact both by affecting the bacterial membrane in a manner that facilitates internalization into the bacterial cell, and subsequently bind to bacterial DNA, thus affecting transcription/replication processes [60,61]. Other types of AMPs, such as the proline-rich bactenecins use transporters to internalize and then bind to ribosomes, inhibiting translation [62]. To test for these possibilities with anisaxins, tests of DNA binding and interference with the ribosome machinery were performed. However, changes to chromosomal DNA during replication or interference with nucleic acids were not observed, up to concentrations several times higher than MIC values (**Figs. S6** and **S7**). Similarly, no secondary effects were noticed with respect to protein synthesis as suggested by the *in vitro* transcription/translation assay on *E. coli* lysates (**Fig. S8**). This suggests that the killing activity of anisaxins does not involve internalization and interference with intracellular bacterial targets.

Given the above considerations, and the fact that helical peptides are most often membranolytic [63,64], we verified the ability of anisaxin peptides to permeabilize the inner membrane of the reference *E. coli* strain at 0.5, 0.25 and 0.125 μM concentrations. All peptides, when tested at 0.5 μM (∼MIC), showed substantial permeabilization, resulting in 85–90% propidium iodide (PI)-positive cells after 15 min post-exposure (Fig. 5). When treated with 0.25 and 0.125 μM (sub-MIC values), a similar behavior was observed after 15 min, however, followed by an apparent drop in % PI-positive cells after 30 and 60 min exposure (**Fig. S9**). This suggests that bacteria can partly recover from exposure to sublethal concentrations of the peptides, in line with time-killing experiments.

Finally, the effect on the bacterial membrane of the two most potent peptides, anisaxins-2S and -2P, was visualized using fluorescence and AFM imaging at concentrations corresponding to 4 × MIC. For both peptides, AFM data suggest that bacteria preserved their characteristic morphology on exposure to the peptide, without evident membrane disruption (Fig. 6), with respect to control (**Fig. S10**). On the other hand, fluorescence images show a strong PI signal (cells stained red) confirming the flow cytometry data, which suggests that while the mode of action is membranolytic it does not cause visible alterations to the membrane surface (at the used imaging resolution). This type of behavior is also typical for the bee venom-derived peptide, melittin, which has been shown to cause strong molecular leakage from both zwitterionic and anionic lipids, while leaving the cell surface apparently

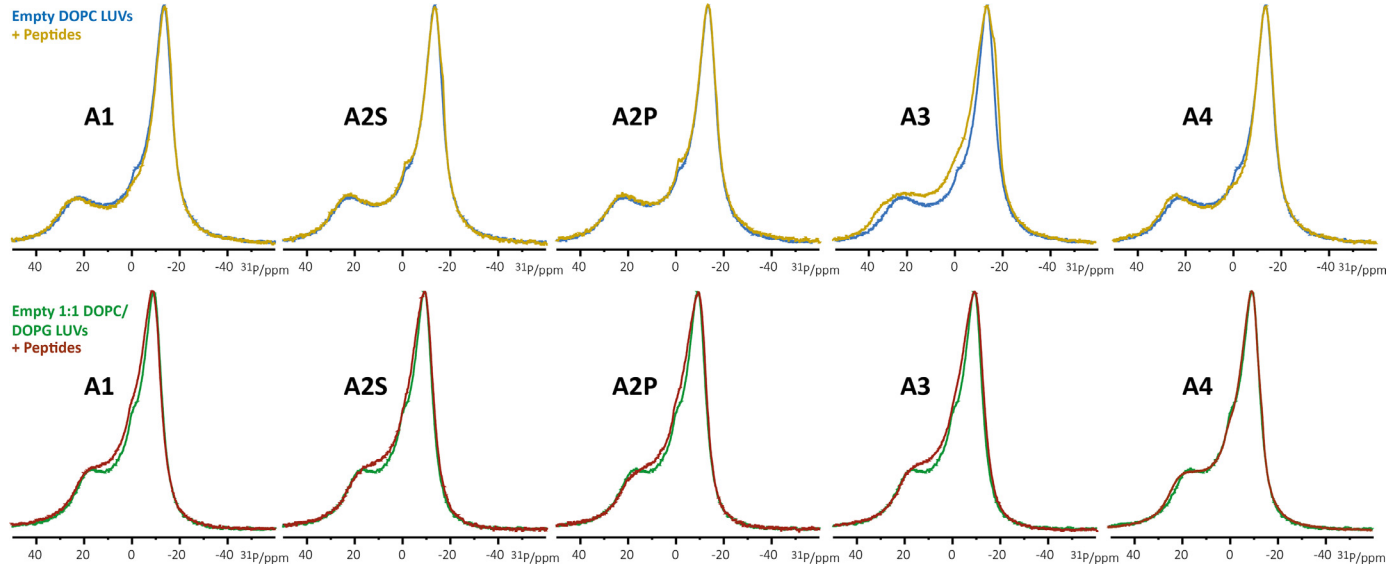

Fig. 4. Static ssNMR ^{31}P spectra of zwitterionic and anionic vesicles in the absence (blue and green) and presence (yellow and red) of anisaxin peptides. All spectra were acquired at 500 MHz (^{1}H frequency).

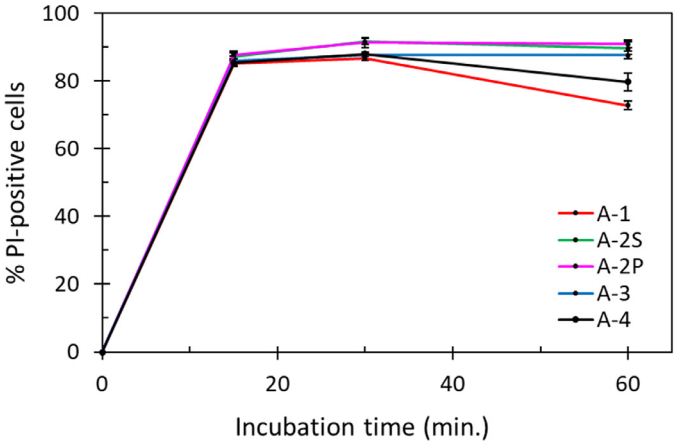

Fig. 5. Evaluation of the effect of anisaxin peptides on *E. coli* ATCC 25922 membrane integrity. Peptides were incubated with *E. coli* ATCC 25922 (1×10^6 CFU/mL) for 60 min at 0.5 μM (generally a MIC). Increase in the signal indicates membrane disruption. Data are expressed as the mean of % PI positive cells ± S.E.M. of three independent experiments.

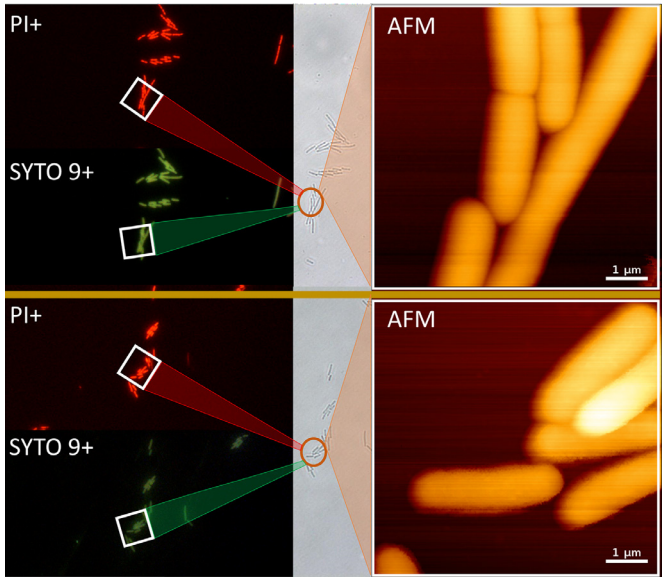

Fig. 6. Fluorescence, bright field (grey) and AFM images of *E. coli* cells treated with anisaxin-2S (upper panel) and -2P (lower panel) at 4 × MIC. AFM data suggest no visible membrane damage. Fluorescence images (PI+, stained in red) confirm membrane disruption.

intact [65]. Furthermore it has been reported to cause similar effects on Gram-positive and Gram-negative bacteria, with a strong PI-induced signal, but minimal or no alternation on the membrane surface [36,66]. For confirmation, we performed additional AFM imaging in ambient conditions of bacteria exposed to all five peptides (see Roncevic et al. [36]), and found that although the membrane surface was left intact, the cell height was considerably reduced (approx. by half) with respect to the control (**Fig. S10**), in line with possible loss of intracellular content.

3.6. Molecular modeling

Further mechanistic insights, that circumvent experimental constraints, were obtained by molecular dynamics (MD) simulations performed on anisaxin-2S (chosen amongst most potent peptides) interacting with a POPE:POPG anionic bilayer modeling the phospholipid composition of an *E. coli* membrane. Interaction of the peptide with the membrane was investigated by imposing different peptide/lipid (P/L) ratios. Strong membrane deformation was observed during the interaction of 12 peptides (P/L = 1/64), positioned in a double star-like manner (Fig. 7) on the membranes surface, where the more closely positioned peptides (inner star), pull up on the membrane, inducing a surface bulge that is mirrored by a concave patch on the inner leaflet (Fig. 7). In this process, some lipids appear to be partially extracted from the membrane, however, since the induced force is not sufficient to completely separate these lipids, the peptides move away from each other, which reduces surface stress and relaxes the membrane. A few of these deformations occur with a decrease in amplitude during a 1 μs simulation time.

On reducing the number of peptides that interact with the membrane to 6 (P/L = 1/128) some fluctuations could still be observed on the membrane, but no initiation of the lipid extraction was observed (**Fig. S11**). This suggests a certain complexity of the molecular mechanism leading to membrane leakage, where a key factor inducing adequate stress on the membrane is a high local surface peptide concentration resulting in a sufficient number of closely spaced peptides. To our knowledge, the involvement of lipid extraction in the mode of action of antimicrobial peptides [67,68] and/or pore-forming proteins [69], is a quite novel mechanism, backed by a recent study of the membranolytic bee venom peptide melittin performed using coarse-grained simulations that are, however, less sensitive compared to all-atom simulations [44,70,71].

3.7. Toxicity and bioavailability

Dose- and time-dependent cytotoxic activity for all peptides tested by differential staining on HPBMCs was only found to be statistically significant in particular cases (Figs. 8 and **S12**). The effect was least pronounced for anisaxin-2S and -2P with >90% and >80% viable cells remaining after 4 h exposure, and >75% viable cells even after 24 h exposure. Treatment with anisaxin-1, -3 and -4 reduced cell viability respectively to 88 ± 3, 70 ± 8 and 75 ± 8 % after 4 h exposure to the highest peptides concentration tested and, in this case, reduced to 44 ± 4, 48 ± 6 and 5 7 ± 8% viable cells after 24 h of exposure to the highest peptides concentration tested. Significantly, the LC_{50} value (i.e., the concentration that reduces the viability of treated cells to 50%) for anisaxin-2S, -2P and -4 was well over 100 μM even for 24 h exposure, and it fell below this value only for anisaxin-1 and -3 (78 and 21 μM, respectively). DNA damage to HPBCs was also determined after exposure to different anisaxins for 4 or 24 using the alkaline comet assay. There was no statistically significant difference in the amount of DNA strand breaks, compared to the corresponding control samples, for any of the tested peptides (Figs. 8 and **S12**).

Given these indications of a relatively low toxicity of anisaxins towards human cells, and particularly the fact that toxicity does not seem to correlate with potency, we tested the pharmacokinetics of the two peptides with the best selectivity indices (LC_{50}/MIC), namely anisaxin-2S and -2P, in a mouse model (**Figs. S13** and **S14**). Both peptides were found to be rather unstable in serum, as their concentrations were below the lower limit of quantification at 30 min post-injection. This is most likely due to the action of serum proteinases, as is commonly reported for linear AMPs [73]. Curiously, at 15 min post-injection anisaxin-2P showed a higher concentration compared to -2S, despite there only being a single residue difference (**Table S2**).

4. Discussion

Transcriptome and genome screening of *A. simplex* and *A. pegreffii* for cecropin-like sequences led to the identification of 14 such

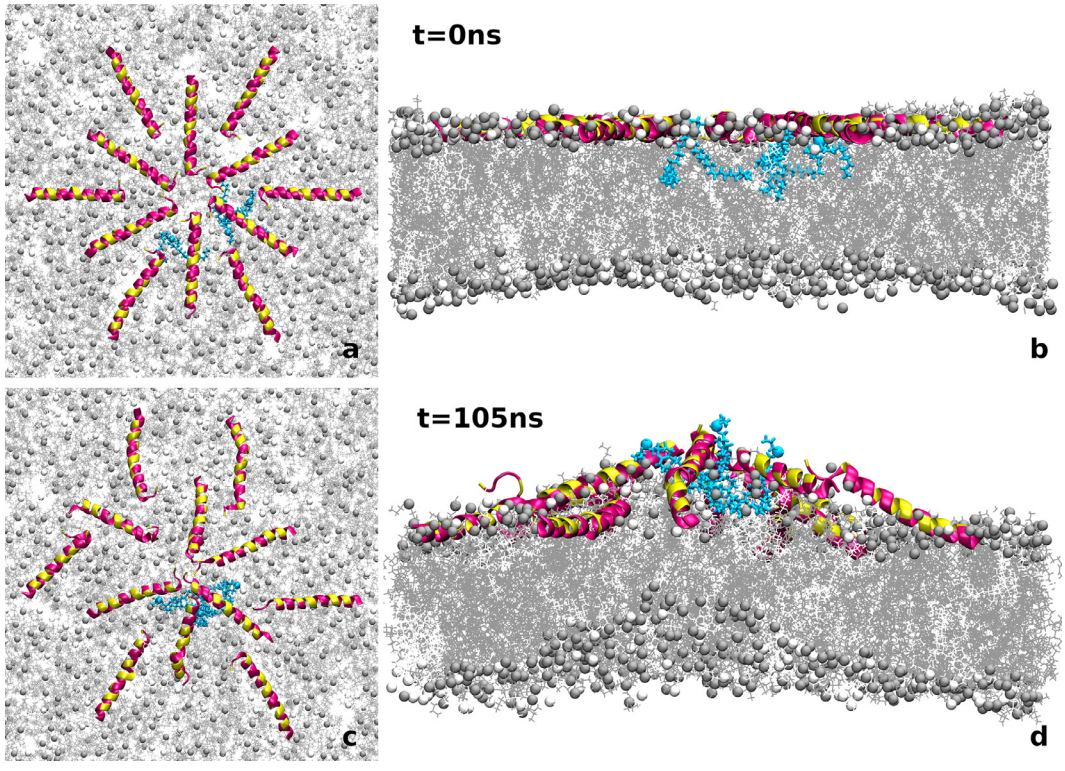

Fig. 7. Simulation of the binding process of twelve anisaxin-2S peptides placed in star-like formation embedded in the polar region of the membrane. The snapshots show top and side view at simulation time 0 ns (a, b) and 105 ns (c, d). At 105 ns, prominent local bulging occurs in both leaflets. Few lipids from the upper leaflet, with the highest separation tendency are highlighted in cyan. The peptide is shown in ribbon representation (yellow - charged residues; magenta - remaining AAs). Membrane lipids are shown in line representation with P atoms shown as beads. Visualization done with VMD [72].

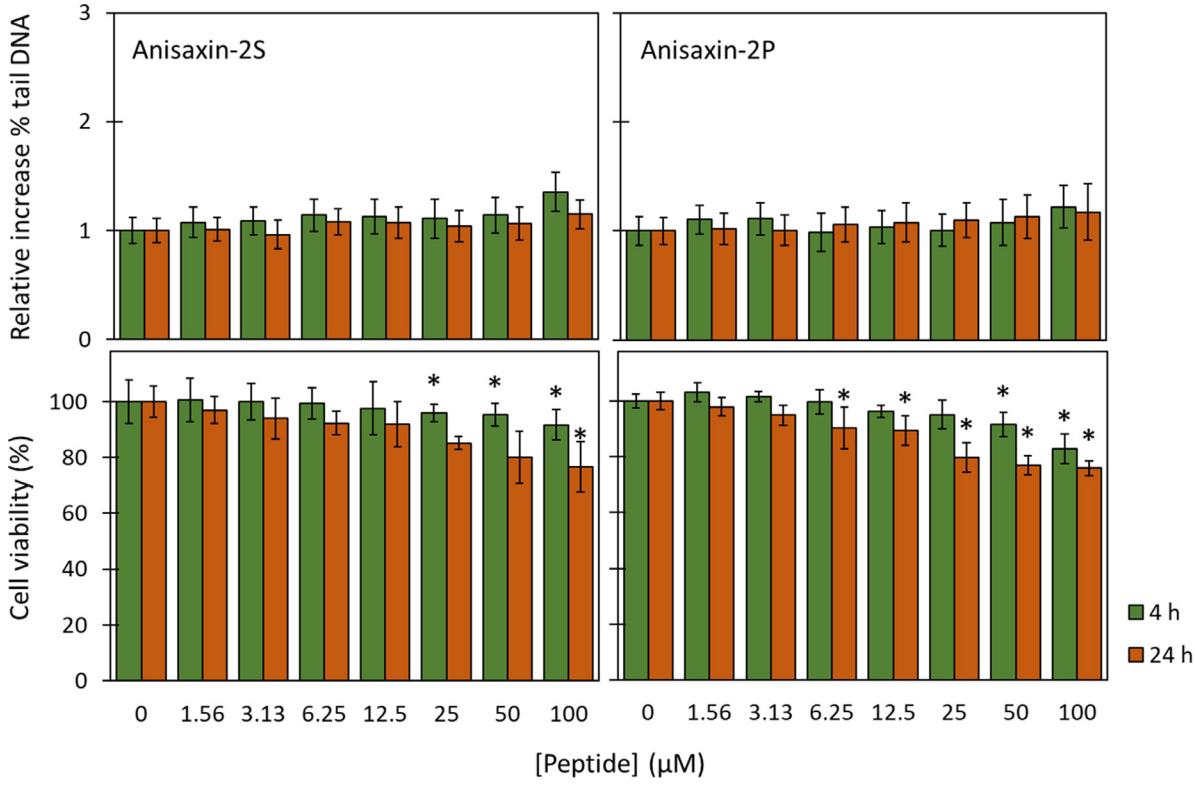

Fig. 8. The effect on cell viability determined by differential staining with acridine orange (AO)/ethidium bromide (EtBr) (lower panel) in human peripheral blood mononuclear cells (HPBMCs) and DNA damage assessed using the alkaline comet assay (upper panel) in human peripheral blood cells (HPBCs) after exposure to different concentrations (0, 1.56, 3.13, 6.25, 12.5, 25, 50 and 100 μM) of anisaxin-2S and -2P for 4 and 24 h. Data are presented as % of the corresponding controls or as the mean % DNA increase in the comet tail for treated cells, over the background level in control cells. Significance of differences was determined with either $\chi 2$-test or Scheffé test ($^*P < 0.05$).

peptides, named anisaxins, where the region corresponding to the mature peptide is well conserved, whereas the N- and C-terminal portions of the precursor sequence is more diverse. This is typical of cecropins and is consistent with reports for peptides from two nematodes that infect terrestrial animals (*T. canis* and *A. suum*).

We found that *A. pegreffii* differentially regulates eight anisaxin peptides in both an accidental host (rat) and a paratenic host (seabass) models (Fig. 1). This is likely due to excretory/secretory products from the parasite's unique excretory gland cell, which is implicated in many biological and physiological processes of the nematode [74]. Interestingly, bacilli aggregations near the cuticle of *Anisakis* larvae perforating the gastric mucosa of rats, occur in association with a conspicuous activation of the interleukin-17 (IL-17) signaling pathway in the rat [75], suggesting the involvement of commensal bacteria in the host's immune response to migrating *A. pegreffii*. This is consistent with our observation that although the expression of anisaxins is similar in migrating (successful infection) and faecally-expelled larvae (unsuccessful infection), suggesting that anisaxins do not necessarily contribute to larval pathogenicity, it is markedly different in the control fish from which larvae were sourced for the experiment (**Table S1**). This suggests that the parasite may increase anisaxins production when exposed to an evolutionary distant microbiome (as in the rat infection model), perceived as more hostile than that of the gastrointestinal tract of the marine animal with which it has co-evolved.

It is also striking that there seems to be a differential expression of specific transcripts in larvae found in different hosts (Fig. 1). The differences in the relative expression levels of anisaxins within the three hosts tested suggests that either specific mechanisms intrinsic to the host contribute to the differential qualitative and quantitative use of particular anisaxins (**Table S1**) or that this may be conditioned by the microbiome composition *in situ*.

Analysis of 14 identified cecropin-like AMP sequences, led to the selection of five non-redundant peptides for structural and functional characterization. These show a moderately amphipathic amino acid arrangement of the mature sequence (**Fig. S5**) centered in the N-terminal, cationic region of the peptides. The overall relative hydrophobic moment (μH^{rel} =0.3–0.35; Table 1) is somewhat lower than what is normally observed for membranolytic helical AMPs (0.5–0.6) [76]. However, the peptides have a conserved tryptophan at position 2 which has been reported to be an important feature for broad-spectrum antimicrobial activity [63,77,78]. Moreover, anisaxins adopt a helical conformation in anisotropic environments, a common feature for many potent AMPs of different origins [7], but to varying degrees. Interestingly, although anisaxins and other cecropin-like peptides identified in insects [63,79] share some biophysical properties with a variety of other AMPs [7] (i.e., a net positive charge and helical amphipathicity), their primary sequence is quite distinct, suggesting they belong to a discrete structural class.

In any case, all anisaxin peptides tested had a potent antimicrobial activity and were selective against Gram-negative bacteria, covering both reference strains and multi-drug resistant isolates. MIC values were in the low micromolar range, sometimes remarkably low (0.25–0.5 μM), and MBCs were similar, suggesting a bactericidal rather than bacteriostatic activity. Their mode of action appears to involve interaction with bacterial membrane and their subsequent rapid permeabilization (15 min or less), even at concentrations below the MBC. Bacteria appear to have the ability to recover from membrane damage up to this threshold concentration at which they are overwhelmed (Figs. 3 and 5).

No visible membrane damage was not observed by AFM after exposure to anisaxins, even at concentrations significantly higher than the MIC or MBC. This is unusual but not unheard of for helical amphipathic AMPs, as the potent and highly membranolytic melittin is reported to act in this manner. Similarities to the mode of action of melittin [70,71] were observed also in MD simulations showing membrane deformation due to peptide-induced surface stress, suggesting lipid extraction as a possible part of their mechanism of action. Such effects depend on the P/L ratio consistent with surface assembly [44], suggesting that the cooperative action of multiple peptides may be required for the antibacterial mechanism. Peptides bind strongly to a negatively charged membrane but have a low tendency to aggregate, so that a large number of peptides are required to produce a sufficiently high local peptide concentration, which induces strong fluctuations in local membrane curvature, leading to unequal stress on the two leaflets. This suggests that the ability of the bacterium to recover from membrane damage at sub-MIC values may be related to its capacity to prevent local accumulation. Otherwise, peptides can lead to lipid extraction, which creates an asymmetry in the number of lipids in the two leaflets. This reduces the free energy barrier for peptide transfer and can lead to transient membrane rupture or peptides insertion and pore formation.

The membrane effects suggested by molecular modeling observations were consistent with an increased permeabilization to PI, a rather small dye, and the reduction in cell height as observed by AFM (**Fig. S10**). It leads us to conclude that it is the peptide-induced molecular leakage of cellular content eventually results in bacterial cell death. The efficient production of membrane lesions that do not result in observable morphological effects represents an important aspect of anisaxins' mode of action, and may be related to the ability of bacteria to recover from the lesions at sub-MIC concentrations. In fact, unlike some other peptides, such as indolicidin, which have a dual mode of action that includes membrane disruption and subsequent inhibition of DNA synthesis [60,61], anisaxins seem to act exclusively by non-specific membrane interactions leading to micro-permeabilization. We did not observe changes to chromosomal DNA during replication or interference with nucleic acids or protein synthesis machinery up to concentrations significantly higher than MIC values (**Figs. S6–S8**).

In most cases, the potent antimicrobial activity of membranolytic AMPs is accompanied by toxic side effects on host cells [54,80]. While the precise endogenous release at sites of infection by the host's immune system is tolerated, exogenous delivery in a therapeutic context leads to unacceptable toxicity. Melittin, a peptide which to some extent has a similar structure and mode of action to anisaxins, is toxic at concentrations comparable to its MIC values [81]. This was not the case for the anisaxin peptides, which showed limited cyto- and genotoxic effect towards HPBMCs and HPBCs, respectively. This extended also to the more potent anisaxin-2S, -2P and -4, for which the particularly low MIC values (often sub-micromolar) contrasted with LC_{50} values well above 100 μM. Anisaxin-1 and -3 were found to be somewhat more toxic, although LC_{50} values were still at least 20 times higher than the bacteriostatic and bactericidal concentrations, for the majority of tested strains (Table 2 and Figs. 8, **S12**). To our knowledge, although the isolation, structure and antibacterial potency of cecropins from other Nematoda (e.g. *A. suum*) have been reported [20,82], toxicity data for these peptides is lacking. Cecropin and cecropin-like AMPs from insects are difficult to compare with, due to significantly different primary sequences in relation to anisaxins, but available data suggest that these have a wide array of activities against animal cells, ranging from inactive to highly toxic so that the sequence of parasitic nematode cecropins may have evolved to result in low cytotoxicity towards animal cells [83].

Based on these encouraging results we carried out preliminary tests on the pharmacokinetics of the two peptides with the best selectivity index (LC_{50}/MIC), namely anisaxin-2S and -2P, in a mouse model (**Figs. S13** and **S14**). Both peptides were unstable *in vivo,* likely due to proteolytic degradation, although the fact

that a single residue difference in anisaxin-2S and -2P increased short-term stability (**Table S2**) with limited detriment to potency or toxicity, suggests that stability can be optimized. Proteolytic degradation is commonly reported for linear AMPs [73], but is not necessarily a major obstacle for their successful application. Potent and non-toxic peptides such as anisaxins might be used for topical external application in their current form, encapsulated within nanocarriers for target-delivery, and/or undergo moderate sequence modifications to improve their stability. The latter approach could be implemented in a number of ways, including the construction of partially or fully enantiomeric peptides, or peptides incorporating non-proteinogenic side-chains in the sequence, or by other structural changes (e.g. cyclization) to prevent proteolysis [84]. This however requires a more detailed understanding of the peptides' mode of action in relation to their structure, as too often quite limited small changes in the primary structure have been found to have profound effects on selectivity. A small effect on selectivity is indeed observed for anisaxin-2S and -2P (e.g., a significantly different activity towards *S. aureus* ATCC, Table 2). In this respect, tools are available to guide sequence variations [85,86].

The high degree of conservation of cecropin-like peptides from parasitic nematodes infecting a wide variety of animal hosts, resulting in potent and selective anti-infective agents, is definitely worth further evaluation. In general, nematodes need to keep the host microbiota in check without harming the host itself, which could explain why they have evolved AMPs with good antibacterial potency but without concomitant toxicity to host cells. The fact that their sequences changed relatively little when some terrestrial hosts adopted a purely marine lifestyle suggests adaptability. Under these conditions the life-cycle of the nematodes evolved to also include infection of invertebrate marine animals (**Fig. S1**), which argues for a certain robustness in the antibacterial activity of the peptides, capable of dealing with entirely diverse microbiotas and environmental conditions.

5. Conclusions

We have identified a group of nematode AMPs from marine parasites of genus *Anisakis* and performed an in-depth characterization of their structural and functional features, with a focus on their antimicrobial activity, their mode of action, their biostability and toxicity. This class of peptides exhibits a potent bactericidal activity, often at sub-micromolar concentrations, with selectivity towards Gram-negative bacteria, including multidrug-resistant strains. Anisaxins have a membranolytic mechanism of action leading to permeabilization, molecular leakage and ultimately cell death, which is rapid. This killing mechanism may be less susceptible to bacterial resistance. As observed by MD simulations, their mechanism of action is very sensitive to local peptide concentration, and may involve significant membrane deformation, such as membrane bulging and lipid extraction. Subsequent stages include membrane lesions that however are not massive, as they do not lead to evident morphological changes to the bacterial surface. There does not seem to be an interaction with intracellular targets. The toxicity of these anisaxins towards host cells was unusually low for AMPs with a membranolytic action, suggesting that at least some of them may have a realistic therapeutic potential for treating human infections, and thus warrant further research. *In vivo* experiments on mice suggest a low stability, making them unsuitable for systemic use in their current form. For this reason, further attention will be devoted to sequence modifications to improve resistance to proteases and to enable successful drug delivery, or to formulation for topical uses. In this respect, the fact that minimal changes in the sequence result in observable difference in the stability, while not greatly affecting activity or toxicity, is encouraging.

Funding

This research was funded by Croatian Science Foundation (project AnisCar: *Anisakis* as a carcinogen: Daring to bust Lancet's myth or revealing its true colors, grant no. IP-2018-01-8490 to I.M.) and EU co-financing and the Interreg V A Italy - Croatia CBC Programme (project AdriAquaNet: Enhancing Innovation and Sustainability in Adriatic Aquaculture, grant no. 10045161 to I.M.).

Declaration of Competing Interest

The authors declare that they have no known competing financial interests or personal relationships that could have appeared to influence the work reported in this paper.

Acknowledgments

The authors would like to thank Prof. Ivana Goić-Barišić and the Laboratory for Clinical Microbiology at the University Hospital Centre Split, Croatia for kindly providing clinical bacterial isolates used in the study. The molecular modeling (MD simulations) was supported by the Center for Advanced Computing and Modeling, University of Rijeka. This manuscript was also part of the research programme of the Netherlands Centre for One Health (www.ncoh.nl) and benefited from access to NMR facility at Bijvoet centre, UU, the Netherlands and has been supported by iNEXT-Discovery, project number 871037, funded by the Horizon 2020 program of the European Commission. This research was partially supported under the project STIM – REI, Contract Number: KK.01.1.1.01.0003, a project funded by the European Union through the European Regional Development Fund - the Operational Programme Competitiveness and Cohesion 2014-2020 (KK.01.1.1.01).

Supplementary materials

Supplementary material associated with this article can be found, in the online version, at doi:10.1016/j.actbio.2022.04.025.

References

[1] F. Prestinaci, P. Pezzotti, A. Pantosti, Antimicrobial resistance: a global multifaceted phenomenon, Pathog. Glob. Health 109 (2015) 309–318, doi:10.1179/2047773215Y.0000000030.

[2] R. Draenert, U. Seybold, E. Grützner, J.R. Bogner, Novel antibiotics: are we still in the pre–post-antibiotic era? Infection 43 (2015) 145–151, doi:10.1007/s15010-015-0749-y.

[3] WHO, in: Global Priority List of Antibiotic-resistant Bacteria to Guide Research, Discovery, and Development of New Antibiotics, WHO, 2017, p. 7.

[4] S.A. Baltzer, M.H. Brown, Antimicrobial peptides – promising alternatives to conventional antibiotics, J. Mol. Microbiol. Biotechnol. 20 (2011) 228–235, doi:10.1159/000331009.

[5] S.C. Park, Y. Park, K.S. Hahm, The role of antimicrobial peptides in preventing multidrug-resistant bacterial infections and biofilm formation, Int. J. Mol. Sci. 12 (2011) 5971–5992, doi:10.3390/ijms12095971.

[6] R.E.W. Hancock, H.G. Sahl, Antimicrobial and host-defense peptides as new anti-infective therapeutic strategies, Nat. Biotechnol. 24 (2006) 1551–1557, doi:10.1038/nbt1267.

[7] T. Rončević, J. Puizina, A. Tossi, Antimicrobial peptides as anti-infective agents in pre-post-antibiotic era? Int. J. Mol. Sci. 20 (2019) 5713, doi:10.3390/ijms20225713.

[8] F.H. Waghu, R.S. Barai, P. Gurung, S. Idicula-Thomas, CAMPR3: a database on sequences, structures and signatures of antimicrobial peptides, Nucleic Acids Res. 44 (2016) D1094–D1097, doi:10.1093/nar/gkv1051.

[9] R. Bruno, M. Maresca, S. Canaan, J.F. Cavalier, K. Mabrouk, C. Boidin-Wichlacz, H. Olleik, D. Zeppilli, P. Brodin, F. Massol, D. Jollivet, S. Jung, A. Tasiemski, Worms' antimicrobial peptides, Mar. Drugs 17 (2019), doi:10.3390/md17090512.

[10] D.T.J. Littlewood, K. Rohde, Marine parasites and the tree of life, in: Marine Parasitology, CABI Publishing, Wallingford, UK, 2005, pp. 6–10.

[11] N.M. Dheilly, J.M. Martínez, K. Rosario, P.J. Brindley, R.N. Fichorova, J.Z. Kaye, K.D. Kohl, L.J. Knoll, J. Lukeš, S.L. Perkins, R. Poulin, L. Schriml, L.R. Thompson, Parasite microbiome project: grand challenges, PLoS Pathog. 15 (2019) e1008028, doi:10.1371/journal.ppat.1008028.

[12] K. Rohde, P.P. Rohde, K. Rohde, The ecological niches of parasites, in: Marine Parasitology, CABI Publishing, Wallingford, UK, 2005, pp. 286–293.

[13] R.M. Maizels, H.H. Smits, H.J. McSorley, Modulation of host immunity by helminths: the expanding repertoire of parasite effector molecules, Immunity 49 (2018) 801–818, doi:10.1016/j.immuni.2018.10.016.
[14] I. Mladineo, J. Hrabar, *Anisakis pegreffii*, Trends Parasitol. 36 (2020) 717–718, doi:10.1016/j.pt.2020.03.004.
[15] J. Hrabar, H. Smodlaka, S. Rasouli-Dogaheh, M. Petrić, Ž. Trumbić, L. Palmer, K. Sakamaki, T. Pavelin, I. Mladineo, Phylogeny and pathology of anisakids parasitizing stranded california sea lions (*Zalophus californianus*) in Southern California, Front. Mar. Sci. 8 (2021) https://www.frontiersin.org/article/10.3389/fmars.2021.636626. accessed March 4, 2022.
[16] A. Jerončić, D. Nonković, A. Vrbatović, J. Hrabar, I. Bušelić, V. Martínez-Sernández, S.A.L. Rocamonde, F.M. Ubeira, S. Jaman, E.Č. Jeličić, M. Amati, M.A.G. Morales, B. Lukšić, I. Mladineo, *Anisakis* Sensitization in the Croatian fish processing workers: behavioral instead of occupational risk factors? PLoS Negl.Trop. Dis. 14 (2020) e0008038, doi:10.1371/journal.pntd.0008038.
[17] Ž. Trumbić, J. Hrabar, N. Palevich, V. Carbone, I. Mladineo, Molecular and evolutionary basis for survival, its failure, and virulence factors of the zoonotic nematode *Anisakis pegreffii*, Genomics 113 (2021) 2891–2905, doi:10.1016/j.ygeno.2021.06.032.
[18] E. Łopieńska-Biernat, Ł. Paukszto, J.P. Jastrzębski, K. Myszczyński, I. Polak, R. Stryiński, Genome-wide analysis of *Anisakis simplex sensu lato*: the role of carbohydrate metabolism genes in the parasite's development, Int. J. Parasitol. 49 (2019) 933–943, doi:10.1016/j.ijpara.2019.06.006.
[19] F.J. Baird, X. Su, I. Aibinu, M.J. Nolan, H. Sugiyama, D. Otranto, A.L. Lopata, C. Cantacessi, The *Anisakis* transcriptome provides a resource for fundamental and applied studies on allergy-causing parasites, PLoS Negl.Trop. Dis. 10 (2016) e0004845, doi:10.1371/journal.pntd.0004845.
[20] A. Pillai, S. Ueno, H. Zhang, J.M. Lee, Y. Kato, Cecropin P1 and novel nematode cecropins: a bacteria-inducible antimicrobial peptide family in the nematode *Ascaris suum*, Biochem. J. 390 (2005) 207–214, doi:10.1042/BJ20050218.
[21] X.Q. Zhu, P.K. Korhonen, H. Cai, N.D. Young, P. Nejsum, G. von Samson-Himmelstjerna, P.R. Boag, P. Tan, Q. Li, J. Min, Y. Yang, X. Wang, X. Fang, R.S. Hall, A. Hofmann, P.W. Sternberg, A.R. Jex, R.B. Gasser, Genetic blueprint of the zoonotic pathogen *Toxocara canis*, Nat. Commun. 6 (2015) 1–8, doi:10.1038/ncomms7145.
[22] T.N. Petersen, S. Brunak, G. von Heijne, H. Nielsen, SignalP 4.0: discriminating signal peptides from transmembrane regions, Nat. Methods 8 (2011) 785–786, doi:10.1038/nmeth.1701.
[23] M.G. Reese, F.H. Eeckman, D. Kulp, D. Haussler, Improved splice site detection in genie, J. Comput. Biol. 4 (1997) 311–323, doi:10.1089/cmb.1997.4.311.
[24] M.G. Grabherr, B.J. Haas, M. Yassour, J.Z. Levin, D.A. Thompson, I. Amit, X. Adiconis, L. Fan, R. Raychowdhury, Q. Zeng, Z. Chen, E. Mauceli, N. Hacohen, A. Gnirke, N. Rhind, F. di Palma, B.W. Birren, C. Nusbaum, K. Lindblad-Toh, N. Friedman, A. Regev, Full-length transcriptome assembly from RNA-Seq data without a reference genome, Nat. Biotechnol. 29 (2011) 644–652, doi:10.1038/nbt.1883.
[25] D.M. Bryant, K. Johnson, T. DiTommaso, T. Tickle, M.B. Couger, D. Payzin-Dogru, T.J. Lee, N.D. Leigh, T.H. Kuo, F.G. Davis, J. Bateman, S. Bryant, A.R. Guzikowski, S.L. Tsai, S. Coyne, W.W. Ye, R.M. Freeman, L. Peshkin, C.J. Tabin, A. Regev, B.J. Haas, J.L. Whited, A tissue-mapped axolotl de novo transcriptome enables identification of limb regeneration factors, Cell Rep. 18 (2017) 762–776, doi:10.1016/j.celrep.2016.12.063.
[26] B. Li, C.N. Dewey, RSEM: accurate transcript quantification from RNA-Seq data with or without a reference genome, BMC Bioinf. 12 (2011) 323, doi:10.1186/1471-2105-12-323.
[27] R: the R project for statistical computing, (n.d.). https://www.r-project.org/(accessed September 9, 2020).
[28] M.I. Love, W. Huber, S. Anders, Moderated estimation of fold change and dispersion for RNA-seq data with DESeq2, Genome Biol. 15 (2014) 550, doi:10.1186/s13059-014-0550-8.
[29] B.J.H. Kuipers, H. Gruppen, Prediction of molar extinction coefficients of proteins and peptides using UV absorption of the constituent amino acids at 214 nm to enable quantitative reverse phase high-performance liquid chromatography−mass spectrometry analysis, J. Agric. Food Chem. 55 (2007) 5445–5451, doi:10.1021/jf0703371.
[30] Y.H. Chen, J.T. Yang, K.H. Chau, Determination of the helix and β form of proteins in aqueous solution by circular dichroism, Biochemistry 13 (1974) 3350–3359.
[31] T. Rončević, G. Gajski, N. Ilić, I. Goić-Barišić, M. Tonkić, L. Zoranić, J. Simunić, M. Benincasa, M. Mijaković, A. Tossi, D. Juretić, PGLa-H tandem-repeat peptides active against multidrug resistant clinical bacterial isolates, Biochim. et Biophys. Acta BBA Biomembr. 1859 (2017) 228–237, doi:10.1016/j.bbamem.2016.11.011.
[32] D. Juretić, Y. Sonavane, N. Ilić, G. Gajski, I. Goić-Barišić, M. Tonkić, M. Kozic, A. Maravić, F.X. Pellay, L. Zoranić, Designed peptide with a flexible central motif from ranatuerins adapts its conformation to bacterial membranes, Biochim. Biophys. Acta BBA Biomembr. 1860 (2018) 2655–2668, doi:10.1016/j.bbamem.2018.10.005.
[33] , Performance standards for antimicrobial susceptibility testing, in: Proceedings of the CLSI Supplement M100, 29th ed., 2019.
[34] M.J. Hope, M.B. Bally, G. Webb, P.R. Cullis, Production of large unilamellar vesicles by a rapid extrusion procedure. Characterization of size distribution, trapped volume and ability to maintain a membrane potential, Biochim. Biophys. Acta BBA Biomembr. 812 (1985) 55–65, doi:10.1016/0005-2736(85)90521-8.
[35] B.M. Fung, A.K. Khitrin, K. Ermolaev, An improved broadband decoupling sequence for liquid crystals and solids, J. Magn. Reson. 142 (2000) 97–101, doi:10.1006/jmre.1999.1896.
[36] T. Rončević, D. Vukičević, N. Ilić, L. Krce, G. Gajski, M. Tonkić, I. Goić-Barišić, L. Zoranić, Y. Sonavane, M. Benincasa, D. Juretić, A. Maravić, A. Tossi, Antibacterial activity affected by the conformational flexibility in glycine–lysine based α-helical antimicrobial peptides, J. Med. Chem. 61 (2018) 2924–2936, doi:10.1021/acs.jmedchem.7b01831.
[37] L. Krce, M. Šprung, T. Rončević, A. Maravić, V. Čikeš Čulić, D. Blažeka, N. Krstulović, I. Aviani, Probing the mode of antibacterial action of silver nanoparticles synthesized by laser ablation in water: what fluorescence and AFM data tell us, Nanomaterials 10 (2020) 1040, doi:10.3390/nano10061040.
[38] M.J. Abraham, T. Murtola, R. Schulz, S. Páll, J.C. Smith, B. Hess, E. Lindahl, GROMACS: high performance molecular simulations through multi-level parallelism from laptops to supercomputers, SoftwareX 1–2 (2015) 19–25, doi:10.1016/j.softx.2015.06.001.
[39] J.B. Klauda, R.M. Venable, J.A. Freites, J.W. O'Connor, D.J. Tobias, C. Mondragon-Ramirez, I. Vorobyov, A.D. MacKerell, R.W. Pastor, Update of the CHARMM all-atom additive force field for lipids: validation on six lipid types, J. Phys. Chem. B 114 (2010) 7830–7843, doi:10.1021/jp101759q.
[40] W.L. Jorgensen, J. Chandrasekhar, J.D. Madura, R.W. Impey, M.L. Klein, Comparison of simple potential functions for simulating liquid water, J. Chem. Phys. 79 (1983) 926–935, doi:10.1063/1.445869.
[41] K. Murzyn, T. Róg, M. Pasenkiewicz-Gierula, Phosphatidylethanolamine-phosphatidylglycerol bilayer as a model of the inner bacterial membrane, Biophys. J. 88 (2005) 1091–1103, doi:10.1529/biophysj.104.048835.
[42] D. Xu, Y. Zhang, Ab initio protein structure assembly using continuous structure fragments and optimized knowledge-based force field, Proteins Struct. Funct. Bioinf. (2012) 1715–1735, doi:10.1002/prot.24065.
[43] J. Lee, X. Cheng, J.M. Swails, M.S. Yeom, P.K. Eastman, J.A. Lemkul, S. Wei, J. Buckner, J.C. Jeong, Y. Qi, S. Jo, V.S. Pande, D.A. Case, C.L. Brooks, A.D. MacKerell, J.B. Klauda, W. Im, CHARMM-GUI input generator for NAMD, GROMACS, AMBER, OpenMM, and CHARMM/OpenMM simulations using the CHARMM36 additive force field, J. Chem. Theory Comput. 12 (2016) 405–413, doi:10.1021/acs.jctc.5b00935.
[44] Y. Miyazaki, S. Okazaki, W. Shinoda, Free energy analysis of membrane pore formation process in the presence of multiple melittin peptides, Biochim. Biophys. Acta BBA Biomembr. 1861 (2019) 1409–1419, doi:10.1016/j.bbamem.2019.03.002.
[45] S. Jo, T. Kim, W. Im, Automated builder and database of protein/membrane complexes for molecular dynamics simulations, PLoS One 2 (2007) e880, doi:10.1371/journal.pone.0000880.
[46] M. Parrinello, A. Rahman, Polymorphic transitions in single crystals: a new molecular dynamics method, J. Appl. Phys. 52 (1981) 7182–7190, doi:10.1063/1.328693.
[47] H.J.C. Berendsen, J.P.M. Postma, W.F. van Gunsteren, A. DiNola, J.R. Haak, Molecular dynamics with coupling to an external bath, J. Chem. Phys. 81 (1984) 3684–3690, doi:10.1063/1.448118.
[48] B. Hess, H. Bekker, H.J.C. Berendsen, J.G.E.M. Fraaije, LINCS: a linear constraint solver for molecular simulations, J. Comput. Chem. 18 (1997) 1463–1472, doi:10.1002/(SICI)1096-987X(199709)18:12(1463::AID-JCC4)3.0.CO;2-H.
[49] U. Essmann, L. Perera, M.L. Berkowitz, T. Darden, H. Lee, L.G. Pedersen, A smooth particle mesh Ewald method, J. Chem. Phys. 103 (1995) 8577–8593, doi:10.1063/1.470117.
[50] N. Atale, S. Gupta, U.C.S. Yadav, V. Rani, Cell-death assessment by fluorescent and nonfluorescent cytosolic and nuclear staining techniques, J. Microsc. 255 (2014) 7–19, doi:10.1111/jmi.12133.
[51] N.P. Singh, M.T. McCoy, R.R. Tice, E.L. Schneider, A simple technique for quantitation of low levels of DNA damage in individual cells, Exp. Cell. Res. 175 (1988) 184–191.
[52] G. Gajski, V. Garaj-Vrhovac, V. Oreščanin, Cytogenetic status and oxidative DNA-damage induced by atorvastatin in human peripheral blood lymphocytes: standard and Fpg-modified comet assay, Toxicol. Appl. Pharmacol. 231 (2008) 85–93, doi:10.1016/j.taap.2008.03.013.
[53] P. Møller, A. Azqueta, E. Boutet-Robinet, G. Koppen, S. Bonassi, M. Milić, G. Gajski, S. Costa, J.P. Teixeira, C. Costa Pereira, M. Dusinska, R. Godschalk, G. Brunborg, K.B. Gutzkow, L. Giovannelli, M.S. Cooke, E. Richling, B. Laffon, V. Valdiglesias, N. Basaran, C. Del Bo', B. Zegura, M. Novak, H. Stopper, P. Vodicka, S. Vodenkova, V.M. de Andrade, M. Sramkova, A. Gabelova, A. Collins, S.A.S. Langie, Minimum information for reporting on the comet assay (MIRCA): recommendations for describing comet assay procedures and results, Nat. Protoc. 15 (2020) 3817–3826, doi:10.1038/s41596-020-0398-1.
[54] G. Gajski, A.M. Domijan, B. Žegura, A. Štern, M. Gerić, I. Novak Jovanović, I. Vrhovac, J. Madunić, D. Breljak, M. Filipič, V. Garaj-Vrhovac, Melittin induced cytogenetic damage, oxidative stress and changes in gene expression in human peripheral blood lymphocytes, Toxicon 110 (2016) 56–67, doi:10.1016/j.toxicon.2015.12.005.
[55] A. Tossi, L. Sandri, A. Giangaspero, New consensus hydrophobicity scale extended to non-proteinogenic amino acids, Peptides 27 (2002) 416.
[56] S.Y. Lau, A.K. Taneja, R.S. Hodges, Synthesis of a model protein of defined secondary and quaternary structure. Effect of chain length on the stabilization and formation of two-stranded alpha-helical coiled-coils, J. Biol. Chem. 259 (1984) 13253–13261.
[57] S.J. Kohler, M.P. Klein, Orientation and dynamics of phospholipid head groups in bilayers and membranes determined from phosphorus-31 nuclear magnetic

resonance chemical shielding tensors, Biochemistry 16 (1977) 519–526, doi:10.1021/bi00622a028.
[58] E. Strandberg, A.S. Ulrich, NMR methods for studying membrane-active antimicrobial peptides, Concepts Magn. Reson. Part A 23A (2004) 89–120, doi:10.1002/cmr.a.20024.
[59] T. Wang, S.D. Cady, M. Hong, NMR determination of protein partitioning into membrane domains with different curvatures and application to the influenza M2 peptide, Biophys. J. (2012), doi:10.1016/j.bpj.2012.01.010.
[60] C. Subbalakshmi, N. Sitaram, Mechanism of antimicrobial action of indolicidin, FEMS Microbiol. Lett. 160 (1998) 91–96, doi:10.1111/j.1574-6968.1998.tb12896.x.
[61] C.H. Hsu, C. Chen, M.L. Jou, A.Y.L. Lee, Y.C. Lin, Y.P. Yu, W.T. Huang, S.H. Wu, Structural and DNA-binding studies on the bovine antimicrobial peptide, indolicidin: evidence for multiple conformations involved in binding to membranes and DNA, Nucleic Acids Res. 33 (2005) 4053–4064, doi:10.1093/nar/gki725.
[62] M. Scocchi, A. Tossi, R. Gennaro, Proline-rich antimicrobial peptides: converging to a non-lytic mechanism of action, Cell. Mol. Life Sci. 68 (2011) 2317–2330, doi:10.1007/s00018-011-0721-7.
[63] H. Sato, J.B. Feix, Peptide–membrane interactions and mechanisms of membrane destruction by amphipathic α-helical antimicrobial peptides, Biochim. Biophys. Acta BBA Biomembr. 1758 (2006) 1245–1256, doi:10.1016/j.bbamem.2006.02.021.
[64] K.A. Brogden, Antimicrobial peptides: pore formers or metabolic inhibitors in bacteria? Nat. Rev. Microbiol. 3 (2005) 238–250, doi:10.1038/nrmicro1098.
[65] M.T. Lee, T.L. Sun, W.C. Hung, H.W. Huang, Process of inducing pores in membranes by melittin, Proc. Natl. Acad. Sci. 110 (2013) 14243–14248, doi:10.1073/pnas.1307010110.
[66] T. Ronč̆ević, L. Krce, M. Gerdol, S. Pacor, M. Benincasa, F. Guida, I. Aviani, V. Čikeš-Čulić, A. Pallavicini, A. Maravić, A. Tossi, Membrane-active antimicrobial peptide identified in *Rana arvalis* by targeted DNA sequencing, Biochim. Biophys. Acta BBA Biomembr. 1861 (2019) 651–659, doi:10.1016/j.bbamem.2018.12.014.
[67] R. Lipkin, T. Lazaridis, Computational studies of peptide-induced membrane pore formation, Philos. Trans. R. Soc. B Biol. Sci. 372 (2017) 20160219, doi:10.1098/rstb.2016.0219.
[68] J.P. Ulmschneider, M.B. Ulmschneider, Molecular dynamics simulations are redefining our view of peptides interacting with biological membranes, Acc. Chem. Res. 51 (2018) 1106–1116, doi:10.1021/acs.accounts.7b00613.
[69] M. Kulma, G. Anderluh, Beyond pore formation: reorganization of the plasma membrane induced by pore-forming proteins, Cell. Mol. Life Sci. (2021), doi:10.1007/s00018-021-03914-7.
[70] J. Hong, X. Lu, Z. Deng, S. Xiao, B. Yuan, K. Yang, How melittin inserts into cell membrane: conformational changes, inter-peptide cooperation, and disturbance on the membrane, Molecules 24 (2019) 1775, doi:10.3390/molecules24091775.
[71] J. Liu, S. Xiao, J. Li, B. Yuan, K. Yang, Y. Ma, Molecular details on the intermediate states of melittin action on a cell membrane, Biochim. Biophys. Acta BBA Biomembr. 1860 (2018) 2234–2241, doi:10.1016/j.bbamem.2018.09.007.
[72] W. Humphrey, A. Dalke, K. Schulten, VMD: visual molecular dynamics, J. Mol. Graph. 14 (1996) 33–38, doi:10.1016/0263-7855(96)00018-5.
[73] S.J. Kang, S.J. Park, T. Mishig-Ochir, B.J. Lee, Antimicrobial peptides: therapeutic potentials, Expert Rev. Anti Infect. Ther. 12 (2014) 1477–1486, doi:10.1586/14787210.2014.976613.
[74] I. Mladineo, J. Hrabar, H. Smodlaka, L. Palmer, K. Sakamaki, K. Keklikoglou, P. Katharios, Functional ultrastructure of the excretory gland cell in zoonotic anisakids (Anisakidae, Nematoda), Cells 8 (2019) 1451, doi:10.3390/cells8111451.
[75] J. Hrabar, Ž. Trumbić, I. Bočina, I. Bušelić, A. Vrbatović, I. Mladineo, Interplay between proinflammatory cytokines, miRNA, and tissue lesions in *Anisakis*-infected Sprague-Dawley rats, PLoS Negl.Trop. Dis. 13 (2019) e0007397, doi:10.1371/journal.pntd.0007397.
[76] I. Zelezetsky, A. Tossi, Alpha-helical antimicrobial peptides—Using a sequence template to guide structure–activity relationship studies, Biochim. Biophys. Acta BBA Biomembr. 1758 (2006) 1436–1449, doi:10.1016/j.bbamem.2006.03.021.
[77] A. Tossi, L. Sandri, A. Giangaspero, Amphipathic, α-helical antimicrobial peptides, Pept. Sci. 55 (2000) 4–30, doi:10.1002/1097-0282.
[78] D. Andreu, R.B. Merrifield, H. Steiner, H.G. Boman, N-Terminal analogs of cecropin A: synthesis, antibacterial activity, and conformational properties, Biochemistry 24 (1985) 1683–1688, doi:10.1021/bi00328a017.
[79] Q. Wu, J. Patočka, K. Kuča, Insect antimicrobial peptides, a mini review, Toxins 10 (2018) 461, doi:10.3390/toxins10110461.
[80] A. Bahar, D. Ren, Antimicrobial Peptides, Pharmaceuticals 6 (2013) 1543–1575, doi:10.3390/ph6121543.
[81] N. Asthana, S.P. Yadav, J.K. Ghosh, Dissection of antibacterial and toxic activity of melittin: a leucine zipper motif plays a crucial role in determining its hemolytic activity but not antibacterial activity, J. Biol. Chem. 279 (2004) 55042–55050, doi:10.1074/jbc.M408881200.
[82] M. Andersson, A. Boman, H.G. Boman, *Ascaris* nematodes from pig and human make three anti-bacterial peptides: isolation of cecropin P1 and two ASABF peptides, Cell. Mol. Life Sci. CMLS 60 (2003) 599–606, doi:10.1007/s000180300051.
[83] D. Brady, A. Grapputo, O. Romoli, F. Sandrelli, Insect cecropins, antimicrobial peptides with potential therapeutic applications, Int. J. Mol. Sci. 20 (2019) 5862, doi:10.3390/ijms20235862.
[84] A.A. Strömstedt, M. Pasupuleti, A. Schmidtchen, M. Malmsten, Evaluation of strategies for improving proteolytic resistance of antimicrobial peptides by using variants of EFK17, an internal segment of LL-37, Antimicrob. Agents Chemother. 53 (2009) 593–602, doi:10.1128/AAC.00477-08.
[85] N. Kamech, D. Vukičević, A. Ladram, C. Piesse, J. Vasseur, V. Bojović, J. Simunić, D. Juretić, Improving the selectivity of antimicrobial peptides from anuran skin, J. Chem. Inf. Model. 52 (2012) 3341–3351, doi:10.1021/ci300328y.
[86] D. Juretić, D. Vukičević, N. Ilić, N. Antcheva, A. Tossi, Computational design of highly selective antimicrobial peptides, J. Chem. Inf. Model. 49 (2009) 2873–2882, doi:10.1021/ci900327a.